ARL-TR-8565● Nov 2018

US Army Research Laboratory

Testing of 0.25-µm Gallium Nitride (GaN) Monolithic Microwave Integrated Circuit (MMIC) Designs

by John E Penn

NOTICES

Disclaimers

The findings in this report are not to be construed as an official Department of the Army position unless so designated by other authorized documents.

Citation of manufacturer's or trade names does not constitute an official endorsement or approval of the use thereof.

Destroy this report when it is no longer needed. Do not return it to the originator.

ARL-TR-8565 ● Nov 2018

US Army Research Laboratory

Testing of 0.25-µm Gallium Nitride (GaN) Monolithic Microwave Integrated Circuit (MMIC) Designs

by John E Penn
Sensors and Electron Devices Directorate, ARL

REPORT DOCUMENTATION PAGE

Form Approved
OMB No. 0704-0188

1. REPORT DATE *(DD-MM-YYYY)*	2. REPORT TYPE	3. DATES COVERED (From - To)
November 2018	Technical Report	15 August 2018–9 October 2018

4. TITLE AND SUBTITLE
Testing of 0.25-µm Gallium Nitride (GaN) Monolithic Microwave Integrated Circuit (MMIC) Designs

5a. CONTRACT NUMBER

5b. GRANT NUMBER

5c. PROGRAM ELEMENT NUMBER

6. AUTHOR(S)
John E Penn

5d. PROJECT NUMBER

5e. TASK NUMBER

5f. WORK UNIT NUMBER

7. PERFORMING ORGANIZATION NAME(S) AND ADDRESS(ES)
US Army Research Laboratory
ATTN: RDRL-SER-E
2800 Powder Mill Road
Adelphi, MD 20783-1138

8. PERFORMING ORGANIZATION REPORT NUMBER
ARL-TR-8565

9. SPONSORING/MONITORING AGENCY NAME(S) AND ADDRESS(ES)

10. SPONSOR/MONITOR'S ACRONYM(S)

11. SPONSOR/MONITOR'S REPORT NUMBER(S)

12. DISTRIBUTION/AVAILABILITY STATEMENT
Approved for public release; distribution is unlimited.

13. SUPPLEMENTARY NOTES

14. ABSTRACT
The US Army Research Laboratory is exploring devices and circuits for RF communications, networking, and sensor systems of interest to Department of Defense applications, particularly for next-generation radar systems. In any communication system that must operate reliably and efficiently in continually crowded spectrums, efficient, high-power broadband monolithic microwave integrated circuit (MMIC) amplifiers are extremely important. MMIC amplifiers offer multiple purposes for communications, networking, radar, and electronic warfare. This report summarizes testing of MMIC designs, using Qorvo's 0.25-µm high-power and efficient gallium nitride on 4-mil silicon carbide process, that were fabricated under a US Air Force Research Laboratory-sponsored wafer run.

15. SUBJECT TERMS
monolithic microwave integrated circuit, MMIC, gallium nitride, GaN, power amplifier, microwave, voltage-controlled oscillator, VCO

16. SECURITY CLASSIFICATION OF:			17. LIMITATION OF ABSTRACT	18. NUMBER OF PAGES	19a. NAME OF RESPONSIBLE PERSON
a. REPORT	b. ABSTRACT	c. THIS PAGE			John E Penn
Unclassified	Unclassified	Unclassified	UU	38	19b. TELEPHONE NUMBER (Include area code) (301) 394-0423

Contents

List of Figures

List of Tables

Acknowledgments

I would like to acknowledge and thank the US Air Force Research Laboratory team, especially Tony Quach, Vipul Patel, and Aji Mattamana, for the design support, computer-aided design support, technical expertise, and fabrication of these gallium nitride circuits for emerging Department of Defense systems and applications. Dana Sturzebecher of Qorvo designed the broadband two-section Wilkinson Coupler (0.5–3 GHz). Khamsouk Kingkeo of the US Army Research Laboratory provided small signal, large signal, and load pull measurements, die photos, assembly of die with large shunt DC bias capacitors, and packaging of the single-stage power amplifier with SubMiniature version A connectors.

1. Introduction

The US Army Research Laboratory (ARL) evaluated and designed efficient, broadband linear high-power amplifiers for future adaptive, multi-mode, radar systems, in addition to other applications such as communications, networking, and electronic warfare (EW). Qorvo (Greensboro, NC) has a high performance 0.25-µm gallium nitride (GaN) fabrication process and a process design kit (PDK) that researchers at ARL used to design efficient, high-power broadband amplifiers, power amplifiers (PAs), and other circuits for future radar, communications, sensor, and EW systems. Testing was performed on designs of monolithic microwave integrated circuits (MMICs) previously submitted for fabrication as part of an effort led by the Air Force Research Laboratory (AFRL). This technical report documents performance of those MMIC designs. Prior technical reports document the design effort.[1–3]

2. High-Power Couplers (GaN)

A lumped-element passive Wilkinson coupler for combining high-power amplifier stages was designed in Qorvo's 0.25-µm GaN on silicon carbide (SiC) process. To increase the power handling of the combiner, an isolation resistor was used instead of the thin film resistors that have better process control. S-parameter measurements show good agreement between simulations and measurements as shown in Fig. 1. Noise in the measurements is mostly due to having a good two-port calibration while using a nominal 50-ohm termination on the uncalibrated third port during measurements. A picture of the actual fabricated die is shown in Fig. 2.

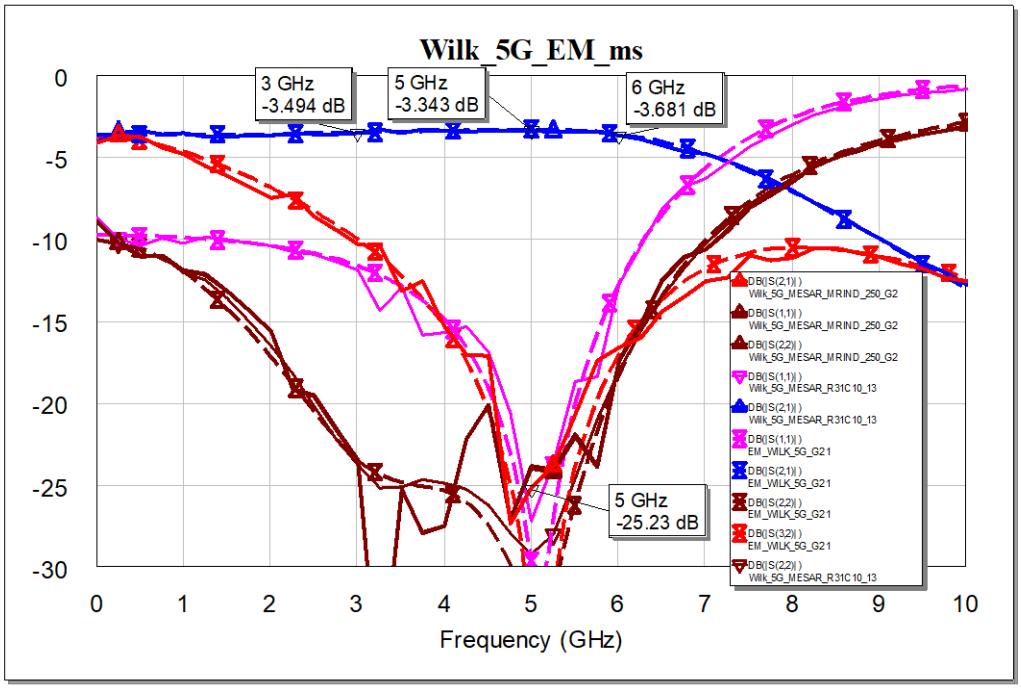

Fig. 1 Measurement (solid) vs. simulations (dash) of 3–6 GHz Wilkinson coupler

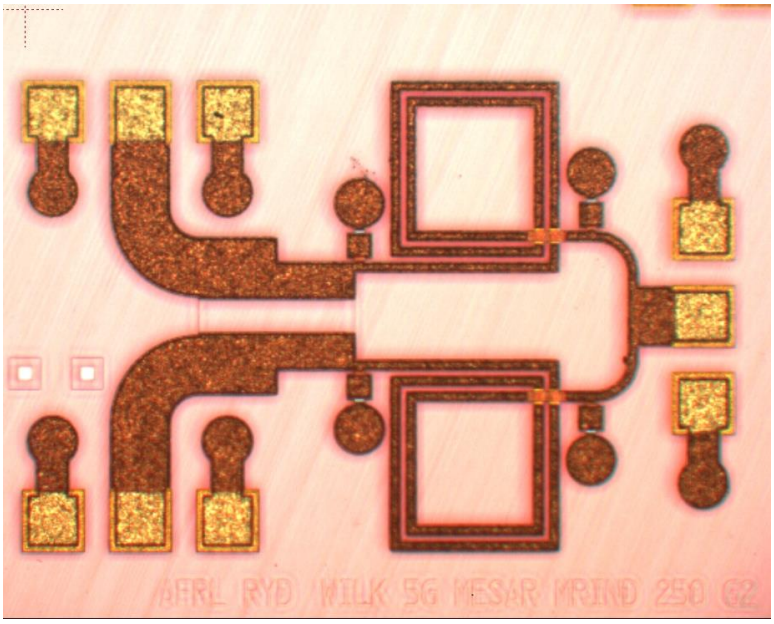

Fig. 2 3–6 GHz Wilkinson coupler GaN MMIC (1.15 × 0.75 mm)

For uses below 3 GHz, another broadband two-section, lumped-element Wilkinson coupler was designed by Dana Sturzebecher of Qorvo. Due to the large 200-µm pitch of the RF ports, and that two of the ports are ground-signal (GS) rather than ground-signal-ground (GSG), this MMIC was wire bonded to Jmicro (J Micro Technology Inc, Portland, Oregon) 150-µm pitch alumina GSG launches. The

additional inductance of the wire bonds for testing, approximately 0.6 to 1 nH, had little impact on the results at these relatively low frequencies. S-parameter measurements show good agreement between simulations and measurements as shown in Fig. 3. Once again, noise in the measurements is mostly due to having a good two-port calibration while using a nominal 50-ohm termination on the uncalibrated third port during measurements. A picture of the actual fabricated die is shown in Fig. 4.

These two high-power passive couplers would need to be packaged to test their power-handling capability, which is expected to be high even for such tiny MMICs.

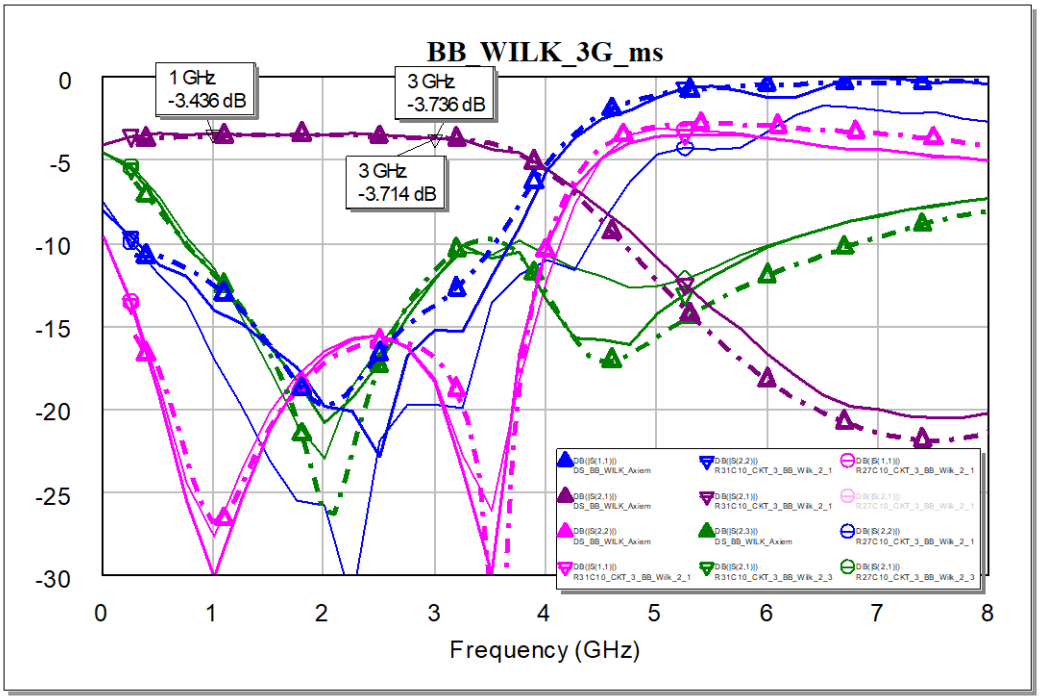

Fig. 3 Measurement (solid) vs. simulations (dash) of broadband 0.5–3 GHz Wilkinson coupler

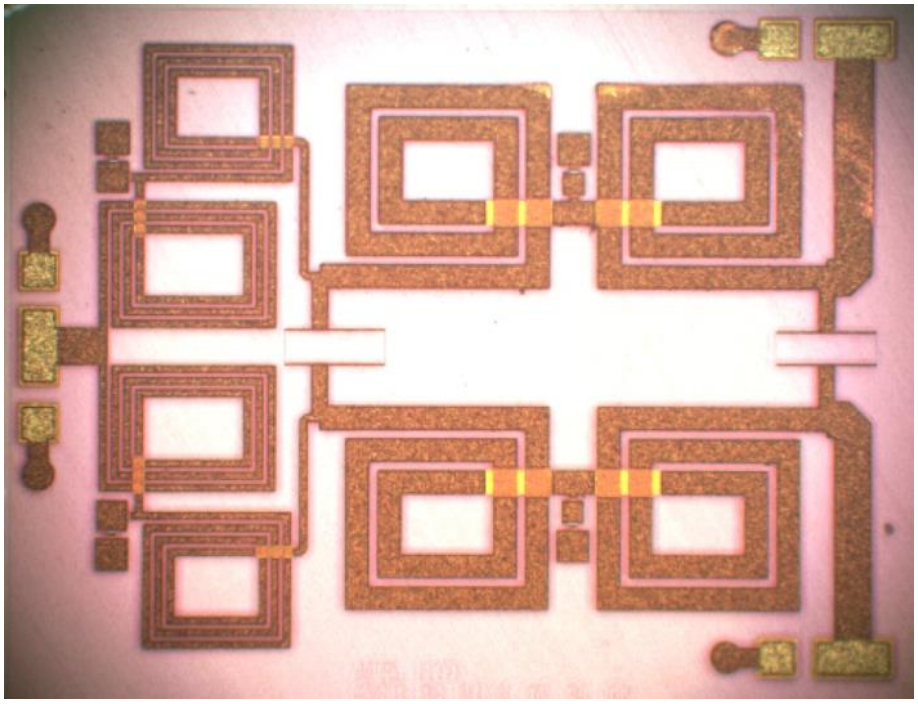

Fig. 4 Broadband 0.5–3 GHz Wilkinson coupler GaN MMIC (2.2 × 1.65 mm)

3. Broadband High-Power Transmit/Receive (TR) Switches (GaN)

A broadband transmit/receive (TR) single-pole, double-throw (SPDT) switch was designed to operate from near DC up to 18 GHz using Qorvo's 0.25-µm GaN on SiC process. The tradeoff of size, topology, and performance resulted in an expected insertion loss of less than 1.5 dB below 16 GHz, with return loss better than 10 dB up to 18 GHz. S-parameter measurements show good agreement between simulations and measurements of the "ON" state with the common "antenna" port connected to one of the two "amplifier" ports (Fig. 5). Ripple in the return loss measurement is due to having a good two-port calibration while using a nominal 50-ohm termination on the uncalibrated third port during measurements. S-parameter measurements show good agreement between simulations and measurements of the "OFF" state with the common "antenna" port connected to the other "amplifier" ports (Fig. 6) with greater than 30 dB of isolation up to 20 GHz. A photo of the actual compact broadband TR switch MMIC is shown in Fig. 7.

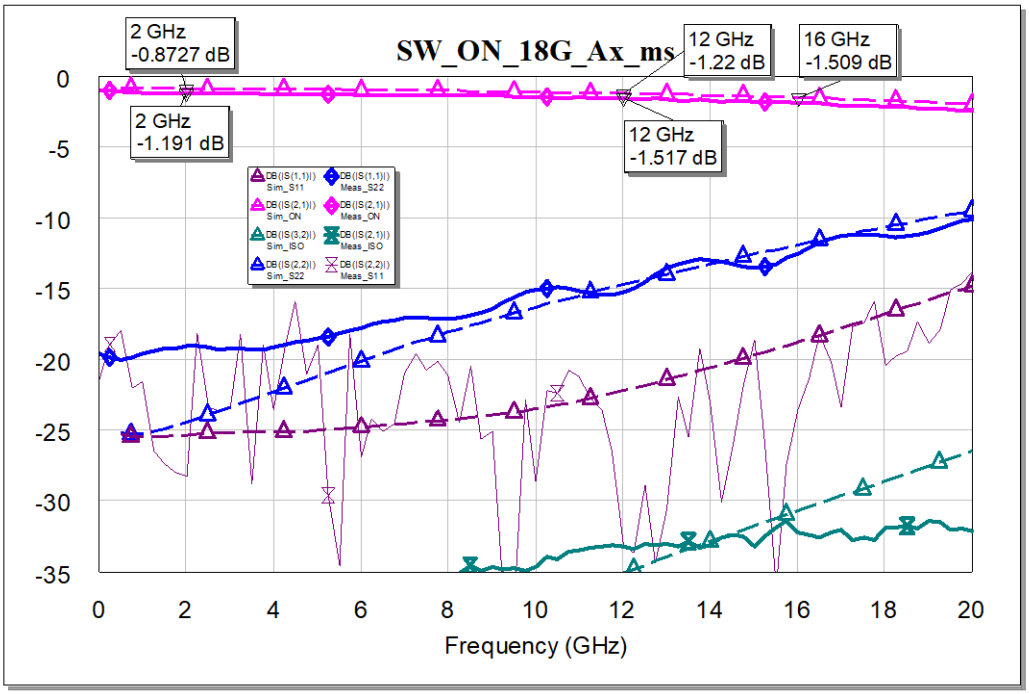

Fig. 5 Measurement (solid) vs. simulations (dash) "ON" broadband 0.3–18 GHz SPDT TR switch

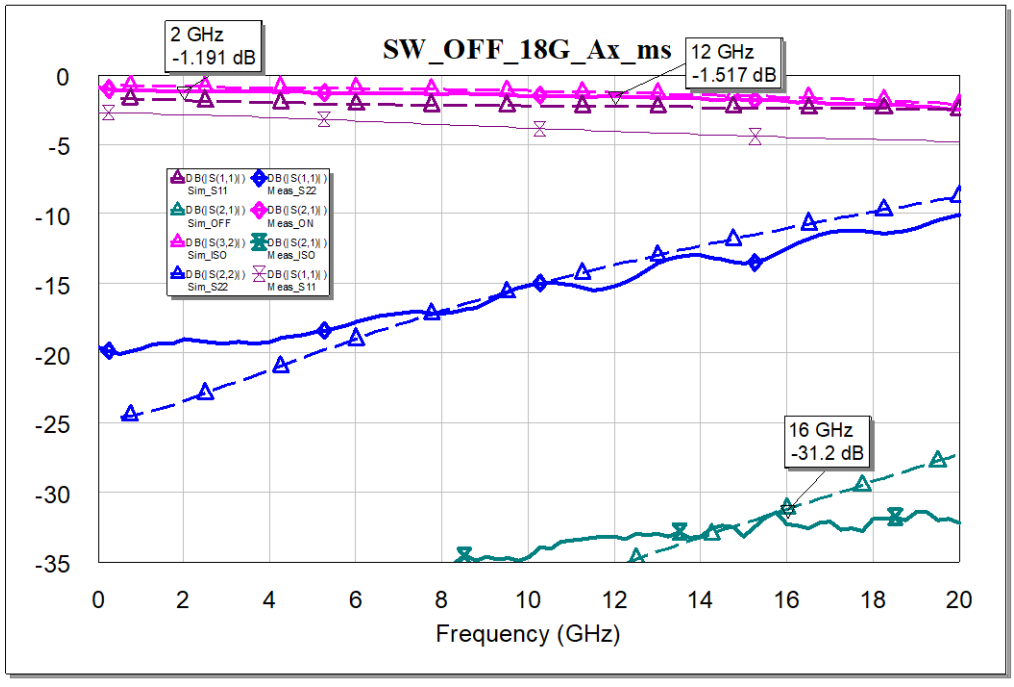

Fig. 6 Measurement (solid) vs. simulations (dash) "OFF" broadband 0.3–18 GHz SPDT TR switch

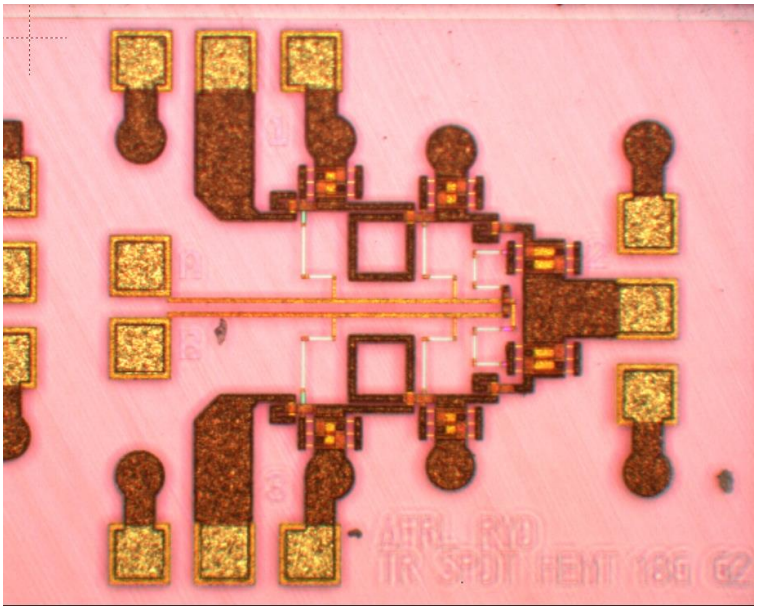

Fig. 7 Broadband 0.3–18 GHz SPDT TR switch GaN 25 µm (0.9 × 0.9 mm)

4. Broadband Distributed Power Amplifier (GaN)

A broadband distributed amplifier (DA) was designed in Qorvo's 0.25-µm GaN on SiC process. S-parameter measurements show good agreement between simulations and measurements of the DA, with good gain up to 25 GHz or so (Fig. 8). Small signal performance at 20 and 28 V with 80 mA current are nearly identical (Fig. 9). Bias tees were used to feed the DC bias at the RF input and output ports, though the gate bias was sometimes fed through a DC bias pad decoupled with a shunt metal-insulator-metal (MIM) capacitor. For testing purposes, the drain bias could likewise be fed through a DC bias pad with shunt MIM capacitor, but would be limited in drain current by the narrow 50-ohm thin film resistor terminating the drain line. A photo of the broadband distributed amplifier MMIC is shown in Fig. 10.

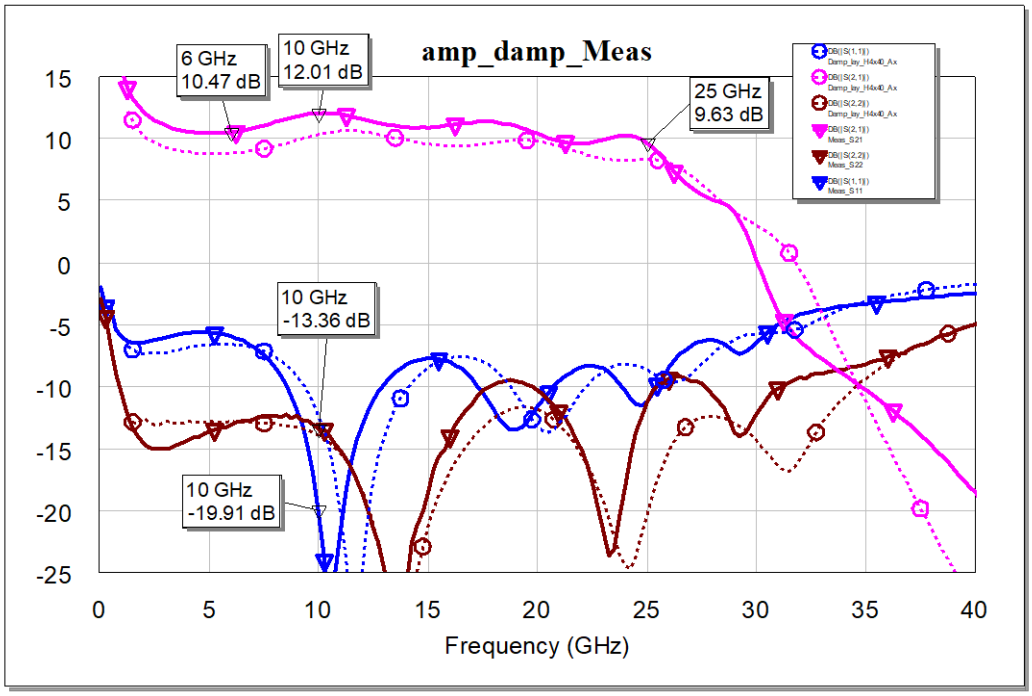

Fig. 8 Measurement (solid) vs. simulations (dash) of broadband distributed amplifier

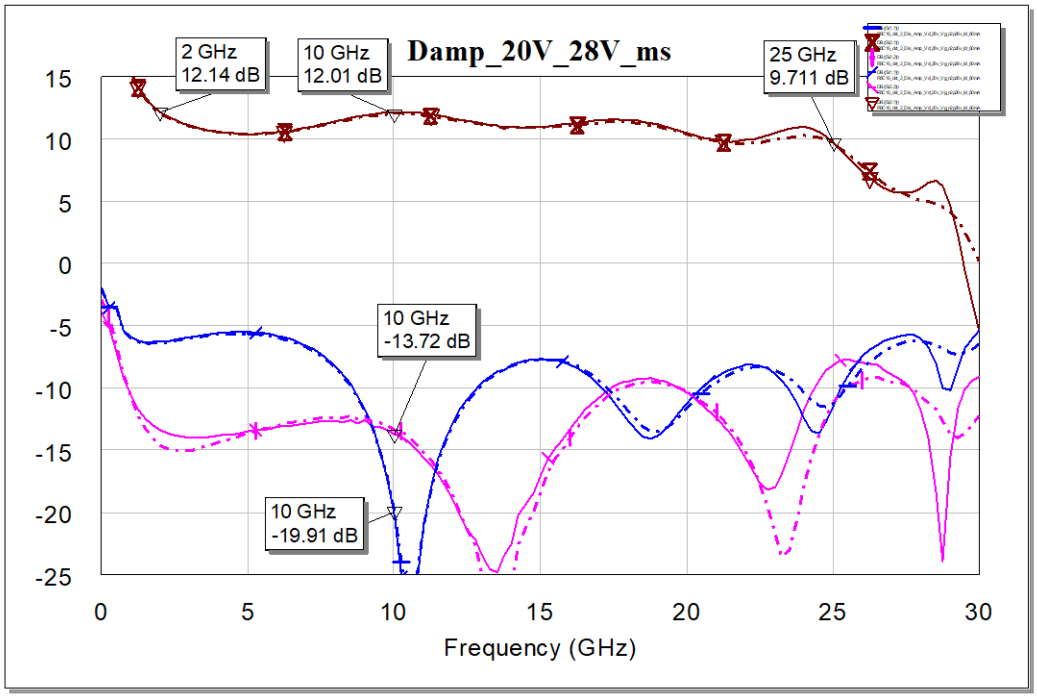

Fig. 9 Measurement of broadband distributed amplifier at 20 V (solid) and 28 V (dash)

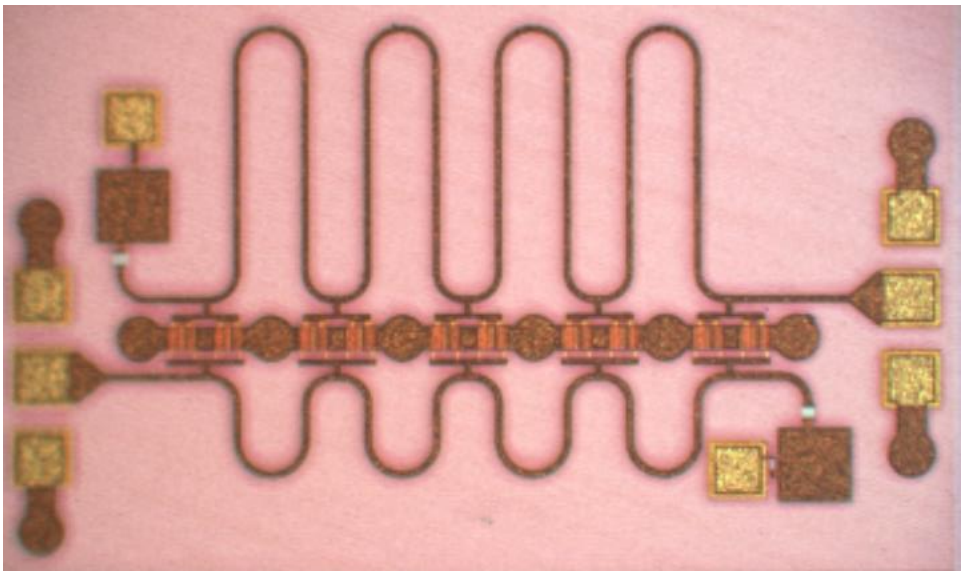

Fig. 10 Broadband distributed amplifier (1.6 × 0.75 mm)

Nonlinear performance of the distributed amplifier was measured at 10, 15, and 20 V with a nominal 80 mA drain current. Output powers were considerably less than expected by 1 to 2 dB. Load pull was performed with slightly better output power or performance using optimized loads that were near 50 ohms. Efficiencies were about as expected with better efficiencies at the lower 10-V bias, while output power increased only slightly with 15- and 20-V bias with generally poorer efficiency. Figure 11 shows a typical plot of output power (power-added efficiency [PAE]) and gain versus input power at 5 GHz and 10 V, while Fig. 12 shows the performance at 20 V. Output powers of 27 dBm (1/2 W) to 28 dBm (5/8 W) were achievable with PAEs around 23% at 10 V, dropping to 13% at 20 V. Nonlinear simulations predicted 29 dBm (0.8 W) to 30 dBm (1 W) with nearly 25% PAE at 10 V, dropping to 15% at 20 V. Measuring unmatched high-electron-mobility transistors (HEMTs) from the same wafer could be helpful in explaining the performance difference between measured and simulated. Small signal gain generally matched better than the nonlinear performance.

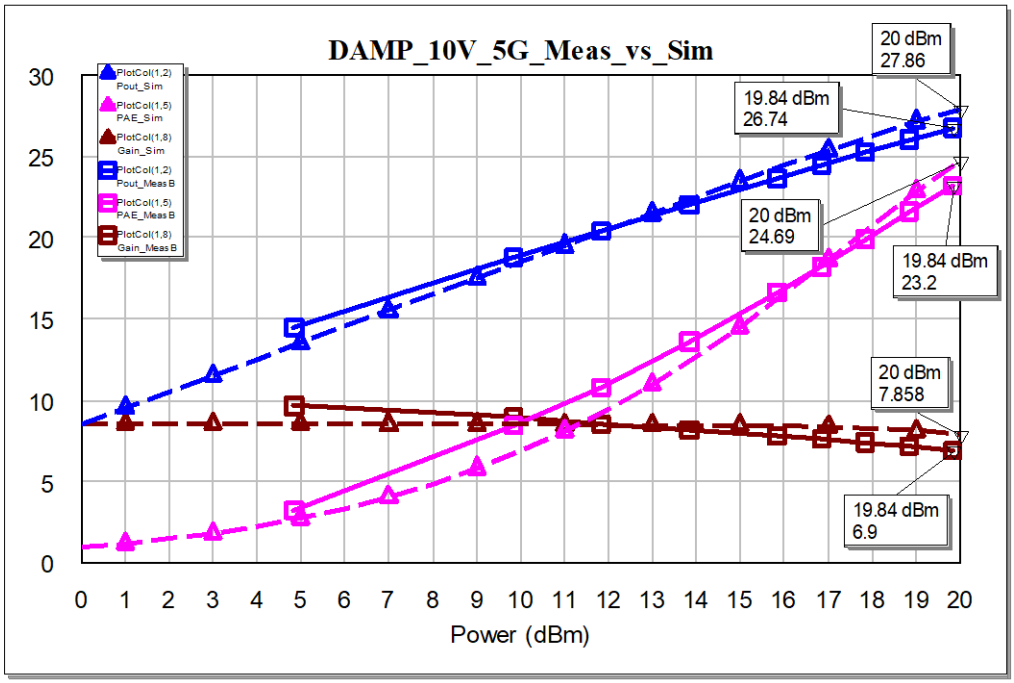

Fig. 11 Measurement (solid) vs. simulations (dash) broadband distributed amplifier (10 V)

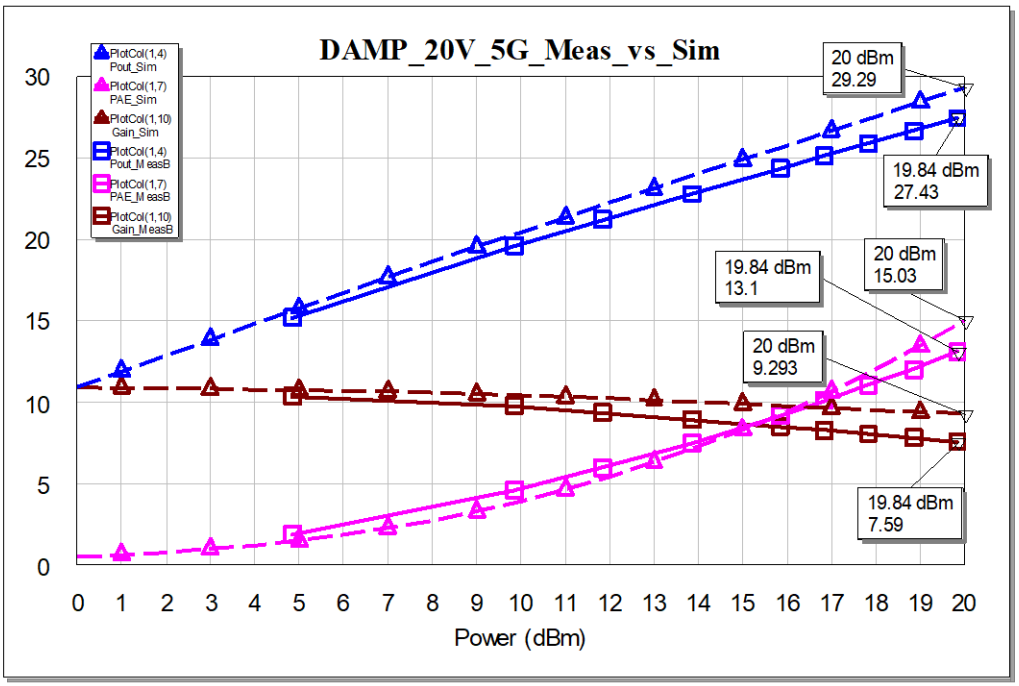

Fig. 12 Measurement (solid) vs. simulations (dash) broadband distributed amplifier (20 V)

5. Voltage-Controlled Oscillator (VCO)

A high-frequency, integrated voltage-controlled oscillator (VCO) design around 15 GHz was designed using the Qorvo 0.25-μm GaN process. An HEMT is used as a variable capacitor (e.g., varactor) to tune the compact GaN VCO. Output power and efficiency are not expected to be high, but the circuit demonstrates the potential for integration and can be supplied over a range of DC biases to tradeoff DC consumption versus performance. Measurements of the output power and oscillation frequency were taken at 12, 15, 17.5, and 20 V while varying the varactor tuning voltage from about –4.5 V to 0 V. Output power was simulated to be about 100 mW, but was closer to 50 mW (17 dBm) at 20 V. Measured output frequency centered around 15 GHz with 500 MHz of tuning range, which matched earlier simulations. Table 1 shows the VCO frequency and output power versus tuning voltage at the nominal 20 V and 40 mA DC bias. There was less power consumption at 17.5 V and 40 mA DC bias, but with a slight shift in frequency (Table 2). A photo of the MMIC is shown in Fig. 13.

Table 1 Measured output frequency and power of VCO (20 V, 40 mA)

Die 1	20V at 40mA		Vg=-2.3V	
VBias (V)	Freq (GHz)	Pout(ms)	Pout(corr)	IDS(mA)
0.0	14.747	-5.2	16.8	40.0
-1.0	14.840	-4.7	17.3	42.0
-2.0	14.933	-4.7	17.3	43.0
-3.0	15.027	-4.7	17.3	44.0
-4.0	15.107	-4.8	17.2	45.0
-4.5	15.267	-5.4	16.6	46.0

Table 2 Measured output frequency and power of VCO (17.5 V, 40 mA)

	17.5V at 40mA		Vg=-2.2V	
VBias (V)	Freq (GHz)	Pout(ms)	Pout(corr)	IDS(mA)
0.0	14.560	-5.6	16.5	40.0
-1.0	14.747	-5.9	16.1	42.0
-2.5	14.827	-5.7	16.3	43.0
-3.5	14.933	-5.8	16.2	44.0
-4.0	15.093	-5.3	16.7	45.0

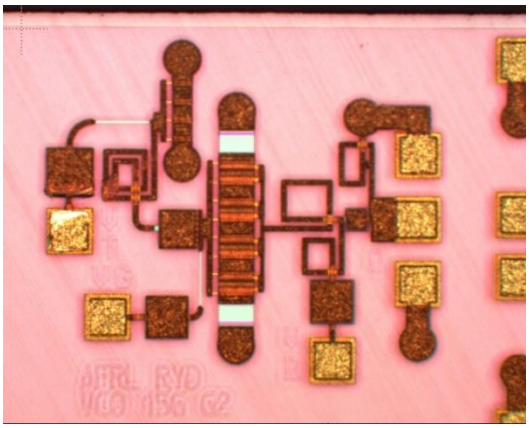

Fig. 13 VCO (0.85 × 0.75 mm)

6. Broadband High-Power Amplifiers

A broadband 3- to 7-GHz one-stage PA was designed in Qorvo's 0.25-µm GaN on SiC process. The die photo of the single-stage amplifier MMIC is shown in Fig. 14. To flatten the gain slope of the PA and increase the compressed gain above 20 dB, a driver stage was added to the one-stage design to create a 3- to 7-GHz two-stage PA. Figure 15 shows the photo of the broadband 3- to 7-GHz two-stage PA. The simple, compact broadband feedback amplifier that serves as the first-stage driver for the two-stage amplifier was submitted for fabrication as a standalone test circuit. Figure 16 shows a photo of the very compact broadband feedback amplifier MMIC for individual tests of the driver stage. The gain of the feedback amplifier has the typical gain rolloff of HEMTs. When used as the driver stage for the two-stage amplifier, additional passive high-pass matching elements were added between the driver stage and the final PA output stage to flatten the gain of the two stage relative to the one-stage 3- to 7-GHz PA.

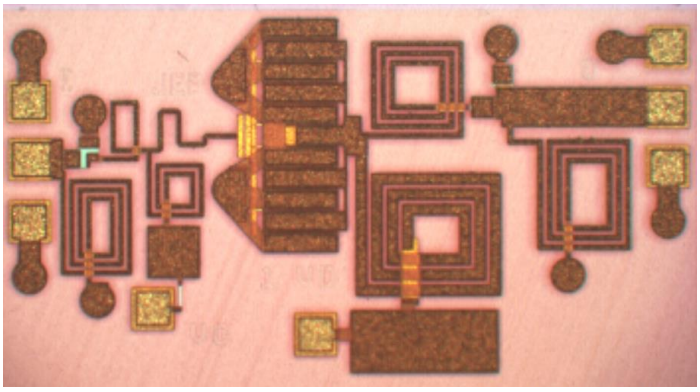

Fig. 14 One-stage (3- to 7-GHz) 1.75-mm GaN HEMT PA (1.6 × 0.8 mm)

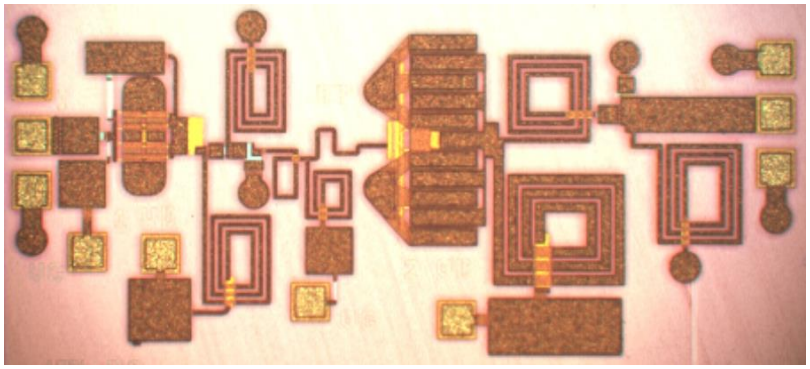

Fig. 15 Two-stage (3- to 7-GHz) 1.75-mm GaN HEMT PA (2.0 × 0.9 mm)

Fig. 16 Standalone broadband feedback amplifier (0.6 × 0.6 mm)

Small signal performance for the one-stage PA matches well from 4 to 7 GHz, except for a measured gain peak at 2.5 GHz and a gain rolloff at the high end at a somewhat lower frequency than expected (Fig. 17). If an additional 50 fF of capacitance between drain and gate (+0.05 pF gate-drain capacitance [Cgd]) is added to the simulation, the high-end gain rolloff and return loss match extremely well with measurements as shown in Fig. 18. It is not clear if this added capacitance indicates a higher than expected Cgd, or if there are some small errors in the electromagnetic (EM) simulations using AWR Axiem and Keysight Momentum software. Measuring test HEMTs from the wafer fabrication may indicate whether this slight shift is due to normal process variation, or if it might be due to some unsimulated parasitic.

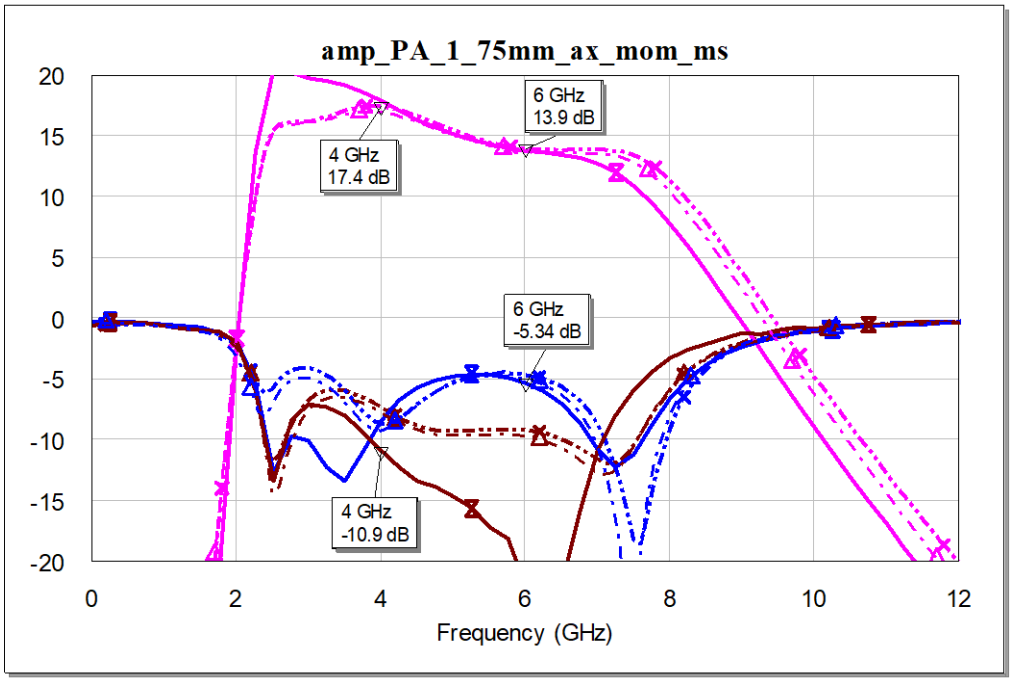

Fig. 17 Measurement (solid) vs. simulations (dash) one-stage 1.75-mm GaN PA

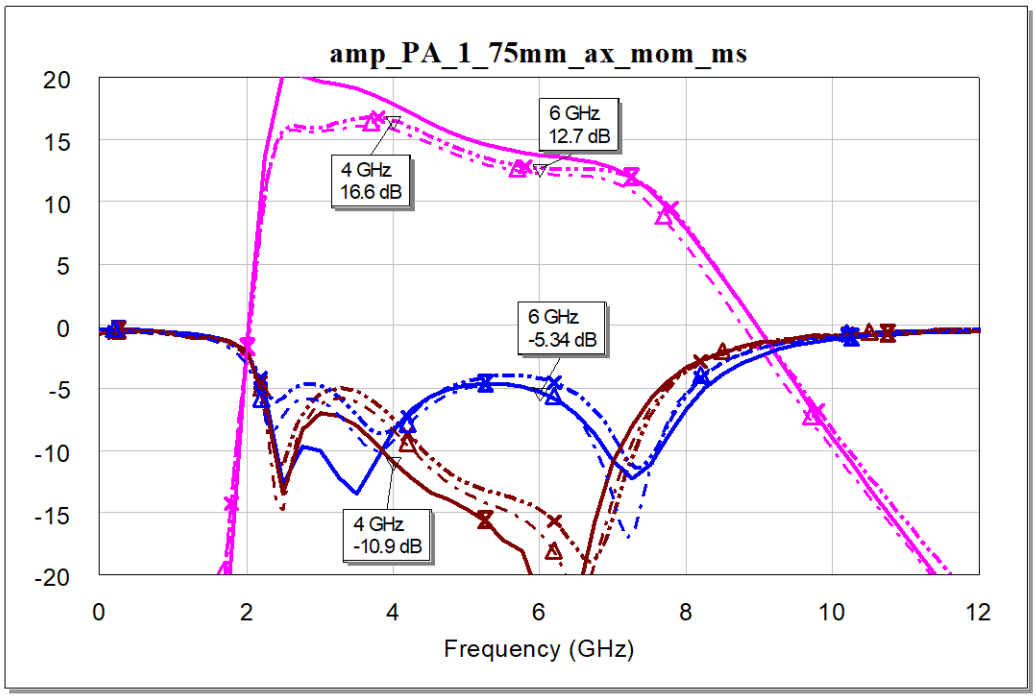

Fig. 18 Measurement (solid) vs. simulations (dash) one-stage 1.75-mm PA (add +0.05 pF Cgd)

Nonlinear performance was measured at 3, 4, 5, 6, and 7 GHz, and 15, 20, and 28 V. Following are plots of output power, PAE, and gain versus input power for 15, 20,

and 28 V, at 4, 5, and 6 GHz. Measured results are solid, while Axiem EM simulations are dotted. In some cases there may be more than one die plotted. Typically, the performance did not vary much between die. Figures 19–21 show nonlinear performance at 4, 5, and 6 GHz, respectively, at a nominal DC bias of 15 V and 50 mA. This is a lower DC bias than the nominal 100 mA/mm bias, which in combination with wire bonds to chip 100 and 1000 pF capacitors at the DC bias pads avoided low frequency oscillations during probe testing. Figures 22–24 show nonlinear performance at 4, 5, and 6 GHz, respectively, at a nominal DC bias of 20 V and 50 mA. While Figs. 25–27 show nonlinear performance at 4, 5, and 6 GHz, respectively, at a nominal DC bias of 20 V and 50 mA. Note the excellent agreement at 5 and 6 GHz, and 20 and 28 V. Generally, there was more discrepancy between measured and modeled at 4 GHz and at the lower 15-V bias, but overall the one-stage amplifier performed close to performance simulations. It should be noted that the design was initially performed with Generation 1 HEMT models for the 0.25-µm GaN process, and when updated Generation 2 HEMT models were used, the output power predictions dropped significantly (1 dB), from 10 W to below 8 W. Based on simulations of the output matching network losses of about 0.6 dB, a measured result of 6.68 W at 52% PAE at 28 V and 4 GHz, translates to 7.7 W and 59.7% PAE at the HEMT for a little more than 4 W/mm of periphery. Table 3 summarizes probe test results for a one-stage 1.75-mm PA (die R28C10) at 15, 20, and 28 V for 4, 5, and 6 GHz.

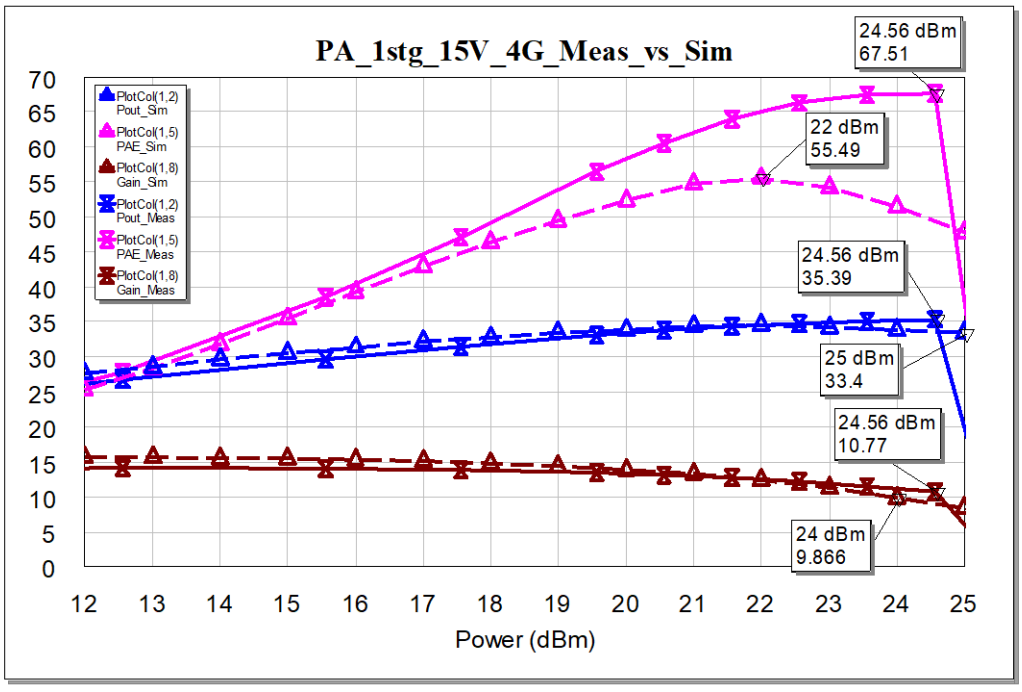

Fig. 19 Measured performance (solid) vs. simulations (dash) one-stage 1.75-mm PA (15 V, 4 GHz)

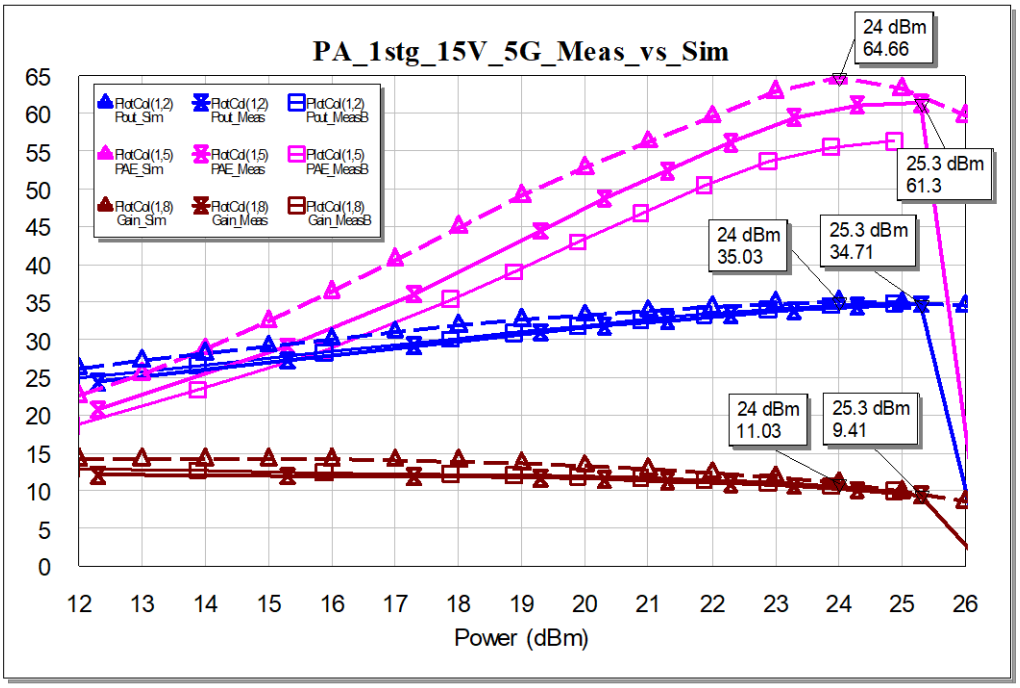

Fig. 20 Measured performance (solid) vs. simulations (dash) one-stage 1.75-mm PA (15 V, 5 GHz)

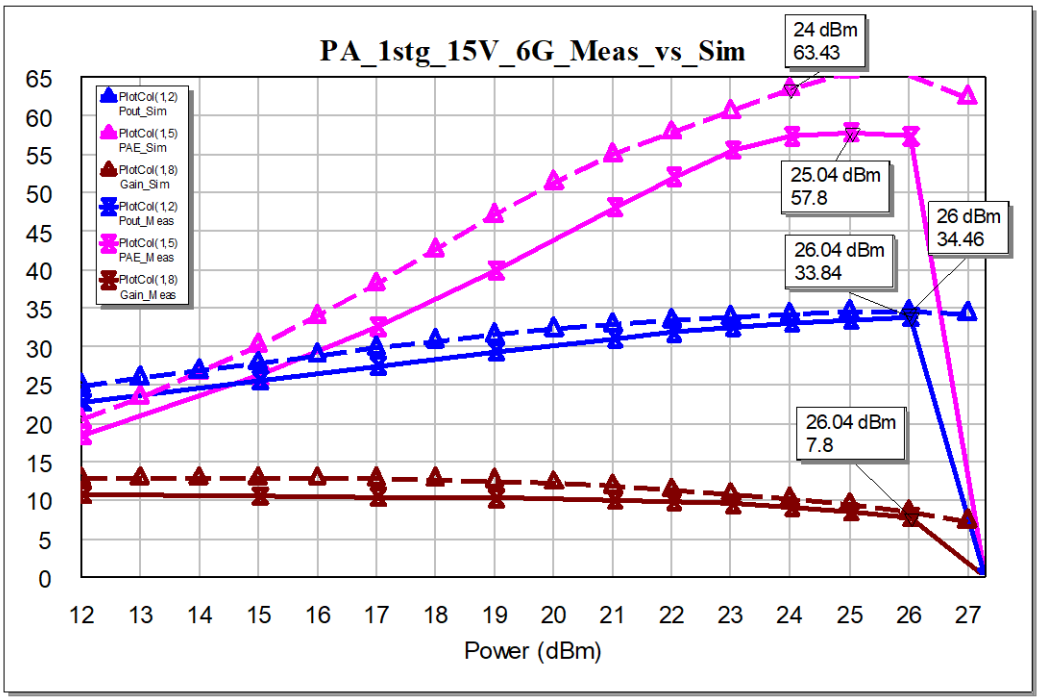

Fig. 21 Measured performance (solid) versus simulations (dash) one-stage 1.75-mm PA (15 V, 6 GHz)

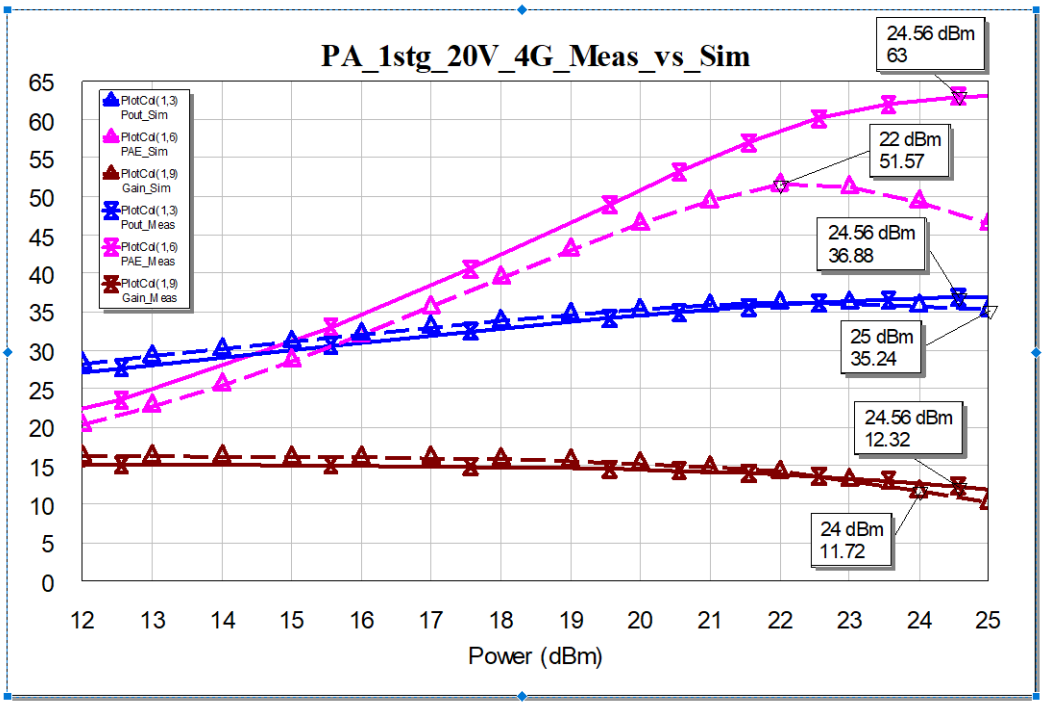

Fig. 22 Measured performance (solid) vs. simulations (dash) one-stage 1.75-mm PA (20 V, 4 GHz)

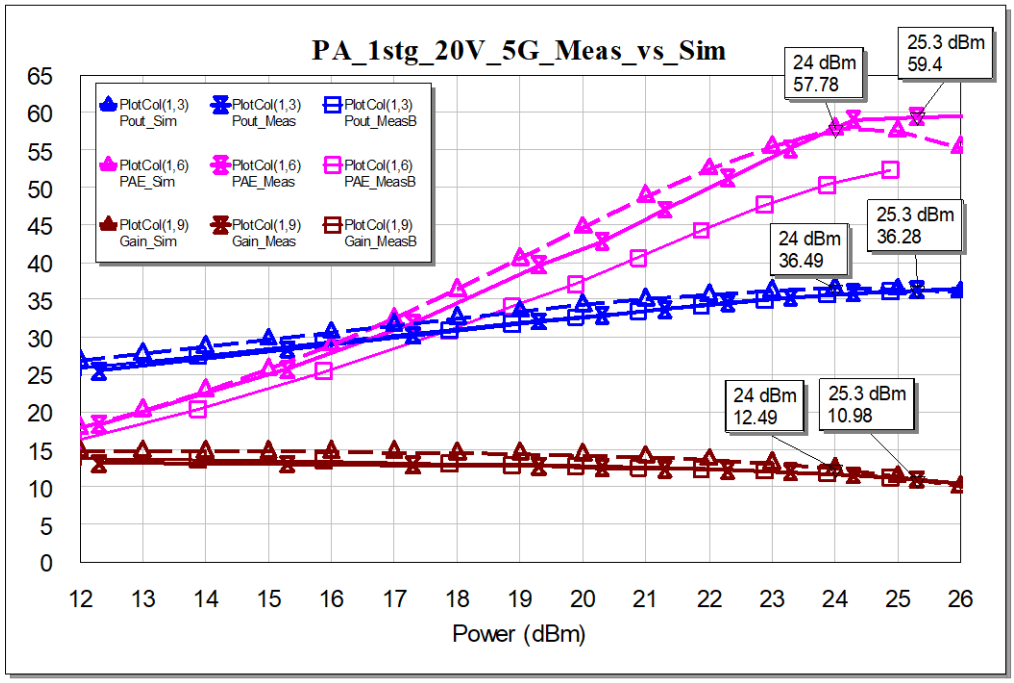

Fig. 23 Measured performance (solid) vs. simulations (dash) one-stage 1.75-mm PA (20 V, 5 GHz)

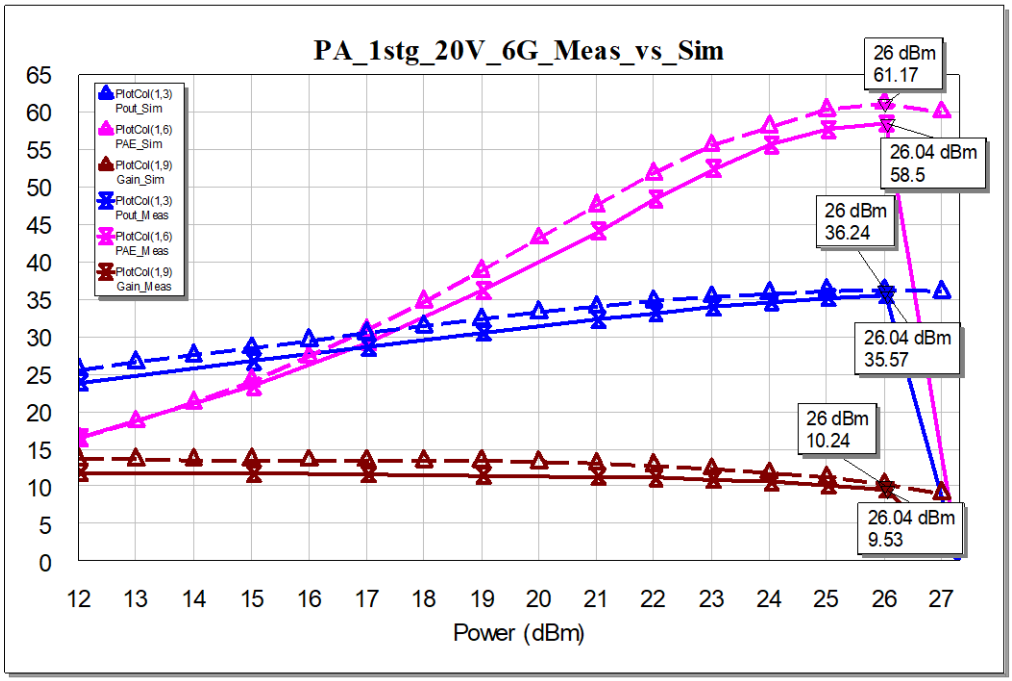

Fig. 24 Measured performance (solid) vs. simulations (dash) one-stage 1.75-mm PA (20 V, 6 GHz)

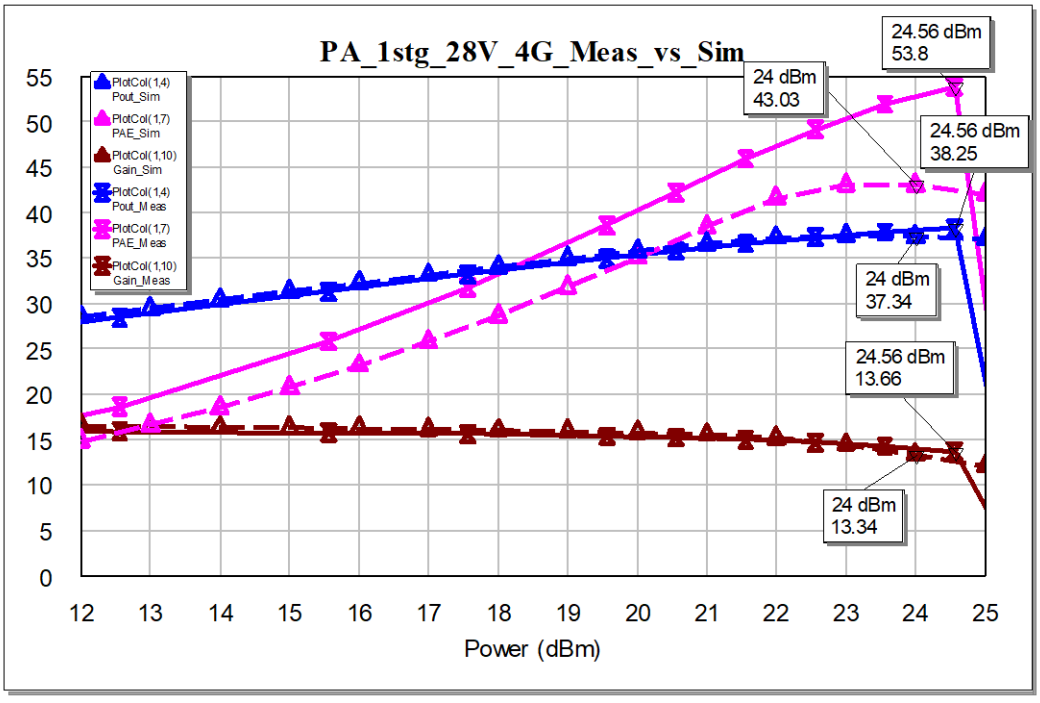

Fig. 25 Measured performance (solid) vs. simulations (dash) one-stage 1.75-mm PA (28 V, 4 GHz)

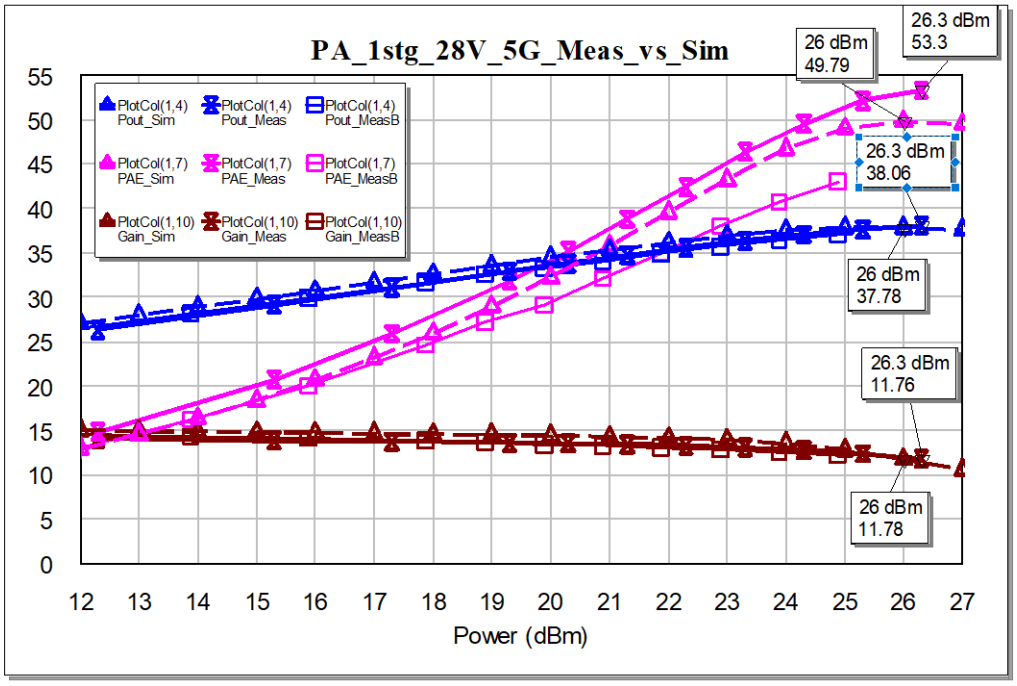

Fig. 26 Measured performance (solid) vs. simulations (dash) one-stage 1.75-mm PA (28 V, 5 GHz)

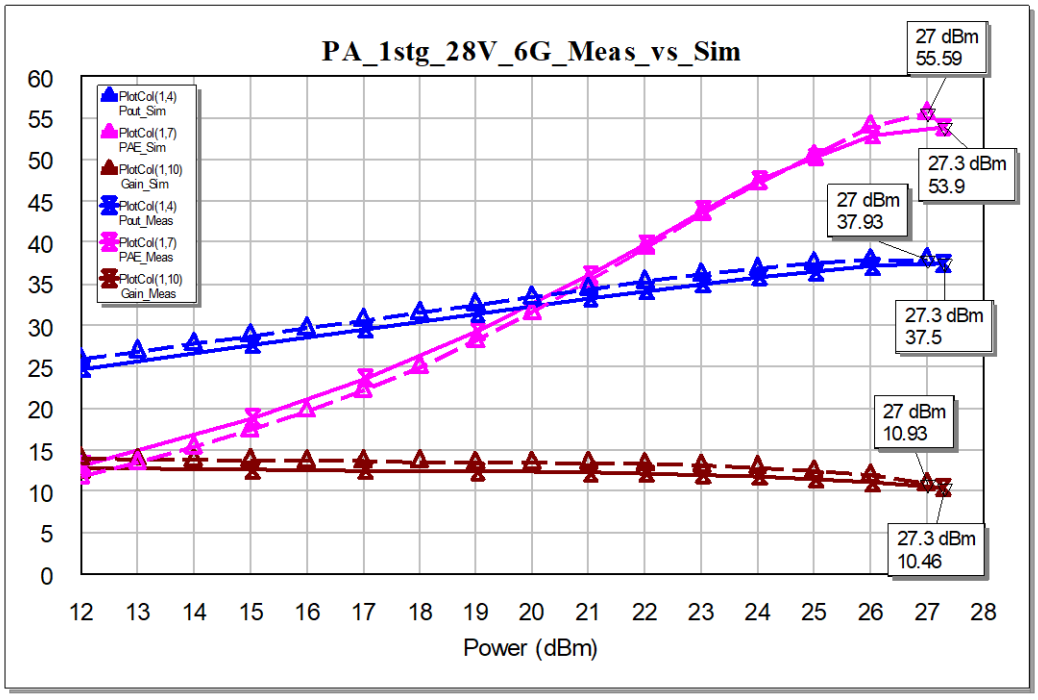

Fig. 27 Measured performance (solid) vs. simulations (dash) one-stage 1.75-mm PA (28 V, 6 GHz)

Table 3 Summary of power performance one-stage 1.75-mm PA

15V									
Freq	Pin	Pout	Gain	Gain Com	Id1	PDC(mw)	Pout(mw)	Drn Eff	PAE
4	27	35.66	11.1	-3.0	329	4935	3681	75	68.8
5	28	34.73	9.43	-2.9	281	4215	2972	71	62.5
6	29	33.84	7.80	-2.9	235	3525	2421	69	57.3
20V									
Freq	Pin	Pout	Gain	Gain Com	Id1	PDC(mw)	Pout(mw)	Drn Eff	PAE
4	28	37.44	11.88	-3.2	397	7940	5546	70	65.3
5	29	36.68	10.38	-2.8	344	6880	4656	68	61.5
6	29	35.64	9.60	-2.2	272	5440	3664	67	60.0
28V									
Freq	Pin	Pout	Gain	Gain Com	Id1	PDC(mw)	Pout(mw)	Drn Eff	PAE
4	27	38.25	13.69	-2.3	425	11900	6683	56	53.8
5	29	38.13	11.83	-2.2	396	11088	6501	59	54.8
6	30	37.68	10.64	-2.1	341	9548	5861	61	56.1

Similarly, the small signal performance for the two-stage PA matches well from 3 to 7 GHz, with slightly flatter gain than expected and with the same gain rolloff at the high end as seen in the one-stage PA. The simulated gain peak (dash) just below 4 GHz is not seen in the measured gain (solid), as shown in Fig. 28. As with the one-stage PA, if an additional 50 fF of capacitance between drain and gate (+0.05 pF Cgd) is added to the simulation, the high-end gain rolloff and output return loss match reasonably well with measurements (Fig. 29). Recall that, as with the one-stage PA, this added capacitance could indicate a higher-than-expected Cgd capacitance, or could be a small error in the EM simulations using AWR Axiem and Keysight Momentum. Measuring test HEMTs from the wafer fabrication may indicate whether this slight shift is due to normal process variation, or if it might be due to some unsimulated parasitic.

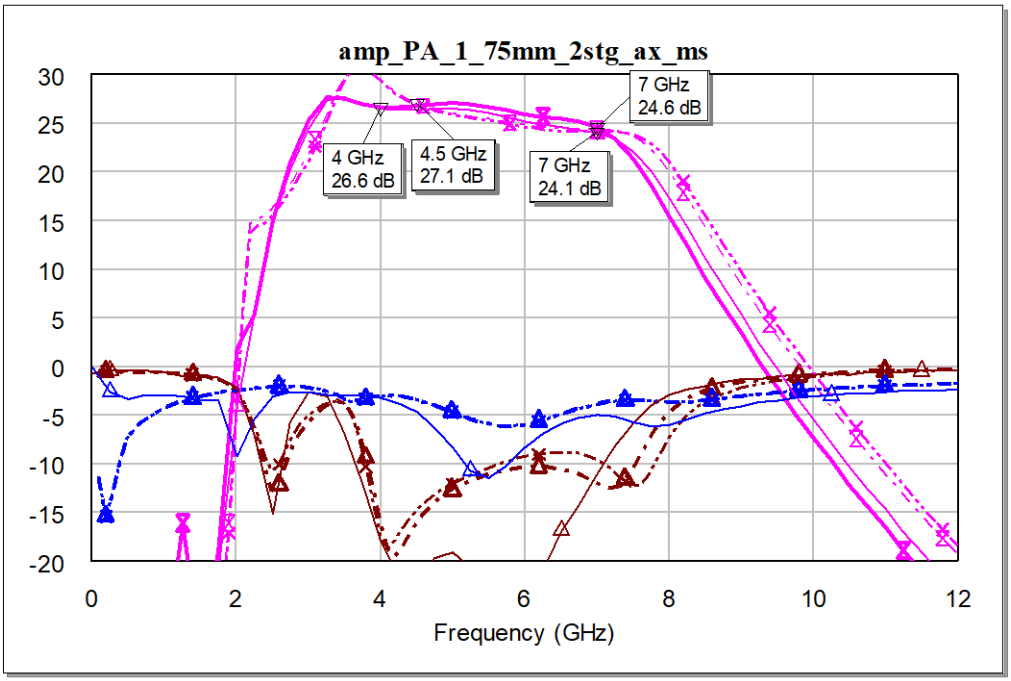

Fig. 28 Measurement (solid) vs. simulations (dash) two-stage 1.75-mm GaN PA

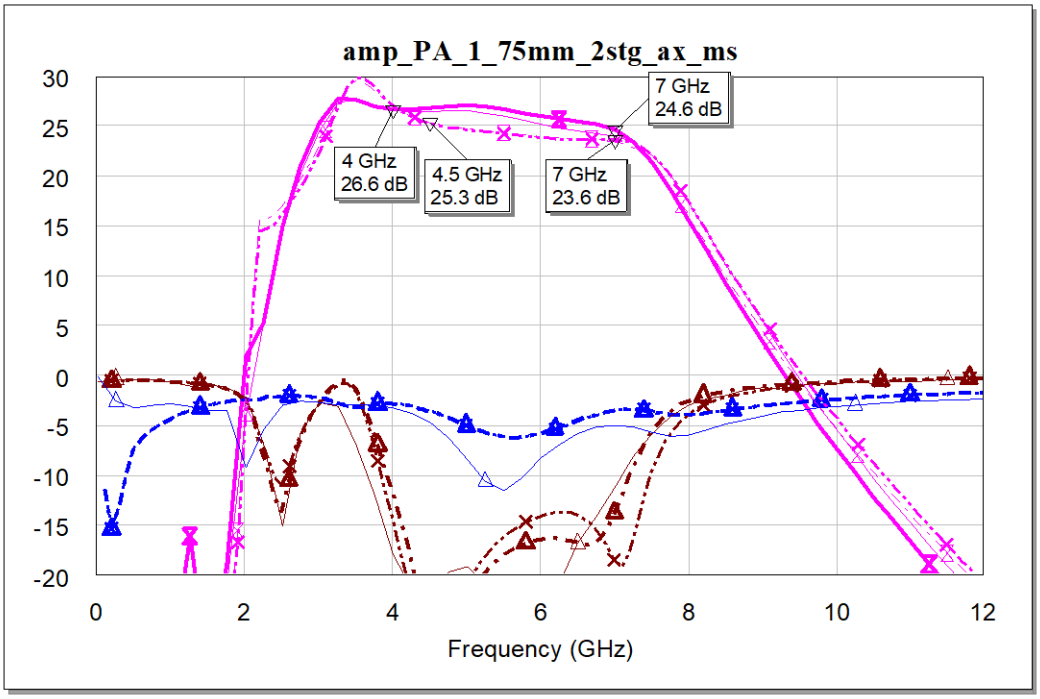

Fig. 29 Measurement (solid) vs. simulations (dash) two-stage 1.75-mm PA (add +0.05 pF Cgd)

Nonlinear performance was measured at 3, 4, 5, 6, and 7 GHz, and 15, 20, and 28 V. The power of the two-stage was less than expected, and later it was discovered that the driver amplifier output power may be significantly lower than expected and is unable to drive the output stage to peak performance. This was confirmed by measuring the standalone feedback amplifier performance, and also measuring the two-stage with separate supplies for the first- and second-stage drains. As both stages were biased class AB, large increases in the first-stage drain current indicated compression in the driver stage. While the one-stage PA had good performance and matched simulations well, the driver stage of the two-stage PA compressed too soon. The simple stable feedback amplifier with high-pass interstage matching elements worked well to flatten the gain with good small signal performance. But, a larger HEMT in the driver stage is needed. If there was a second fabrication, the driver stage output power margins would be increased. The DC power consumption of the driver stage reduces the PAE of the two-stage design, but it performed well over part of the band. Overall, the two-stage performance had good gain and reasonable PAE, with almost 6 W of output power at 28 V and 5 GHz. Table 4 summarizes probe test results for a two-stage 1.75-mm PA at 15, 20, and 28 V for 4, 5, and 6 GHz.

Table 4 Summary of power performance two-stage 1.75-mm PA

15V									
Freq	Pin	Pout	Gain	Gain Com	Id1	PDC(mw)	Pout(mw)	Drn Eff	PAE
4	16.64	35.25	18.62	-4.8	398	5970	3350	56.1	55.3
5	16.40	34.04	17.7	-5.1	306	4590	2535	55.2	54.3
6	18.08	33.14	15.04	-5.9	304	4560	2061	45.2	43.8
20V									
Freq	Pin	Pout	Gain	Gain Com	Id1	PDC(mw)	Pout(mw)	Drn Eff	PAE
4	15.64	35.84	20.2	-3.9	405	8100	3837	47.4	46.9
5	19.45	36.72	17.27	-6.8	420	8400	4699	55.9	54.9
6	18.08	34.86	16.78	-5.2	340	6800	3062	45.0	44.1
28V									
Freq	Pin	Pout	Gain	Gain Com	Id1	PDC(mw)	Pout(mw)	Drn Eff	PAE
4	15.64	36.56	20.92	-3.7	430	12040	4529	37.6	37.3
5	17.32	37.71	20.41	-4.5	427	11956	5902	49.4	48.9
6	22.02	36.81	17.75	-5.2	406	11368	4797	42.2	41.5

The small signal performance for the 0.44-mm broadband feedback driver amplifier matches well with simulations as seen in Fig. 30. Measured results at 10, 20, and 28 V of bias is compared to the simulation (28 V) in Fig. 31. The 10 V measurements are closer to the simulations at 28 V, though there is small variation with bias. It was not expected to be very efficient, but it was simple, very compact, stable, and appeared to produce more than the 1/2 W needed to drive the 1.75-mm PA stage, with simulations predicting 1 W (30 dBm). Unfortunately, the driver amp

was about 1–2 dB lower than expected and compressed before it had sufficient drive for the two-stage amplifier. Granted, there is a small difference in the standalone fabricated broadband feedback amplifier and "as implemented" with the extra high-pass filter elements to flatten the two-stage gain. However, it was very useful to test the individual one-stage driver and one-stage PA, as well as the two-stage PA.

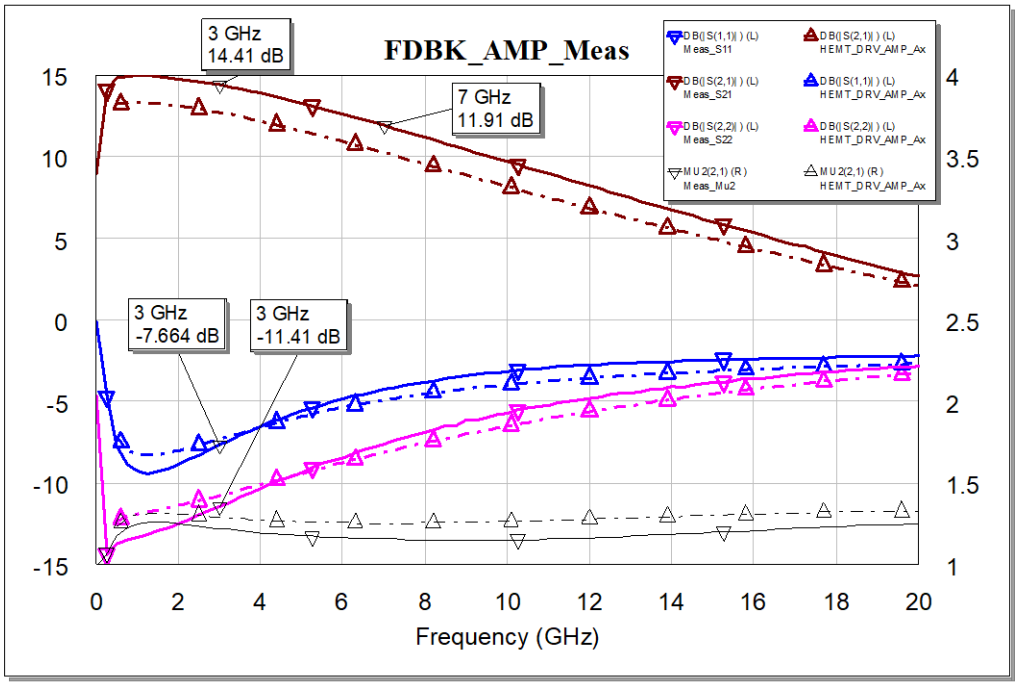

Fig. 30 Measurement (solid) vs. simulations (dash) 0.44-mm broadband feedback driver amp

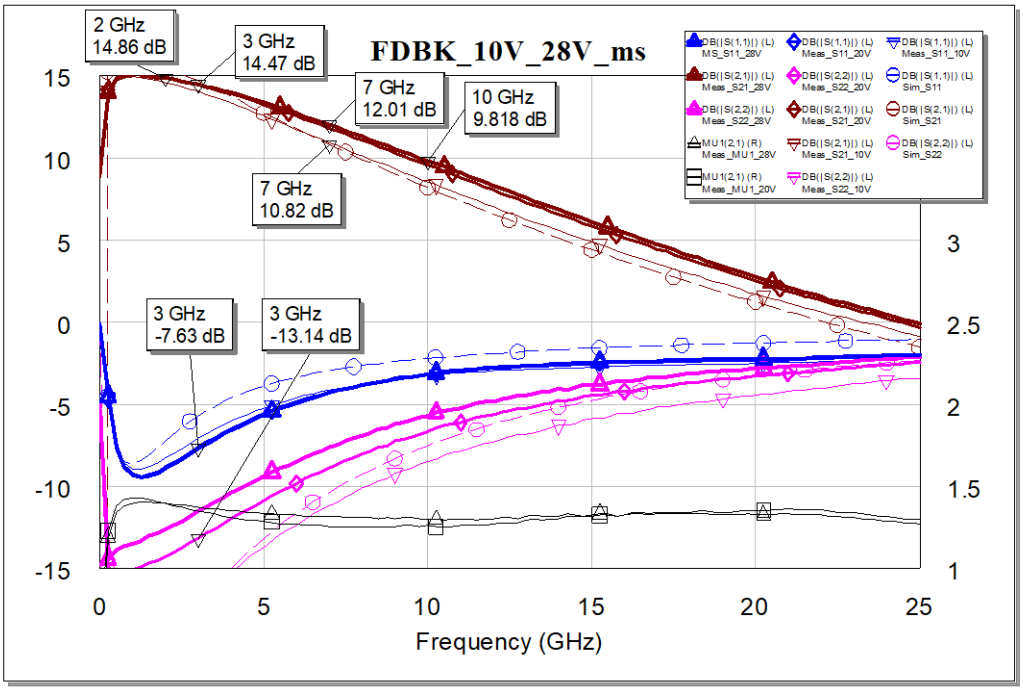

Fig. 31 Measurements 10–28 V (solid) vs. simulations 28 V (dash) 0.44-mm driver amp

Nonlinear performance of the broadband feedback amplifier was measured at 10, 15, 20, and 28 V with a nominal 40-mA drain current. Similar to the distributed amplifier, output powers were considerably less than expected by 1–2 dB. Load pull was performed with better output power or performance using optimized loads, but compromises in performance might be expected over such a broadband. Efficiencies were somewhat lower than expected, yielding better efficiencies at the lower 10-V bias, while output power increased only slightly with 15-, 20-, and 28-V bias resulting in lowering efficiencies at higher voltages. Figure 32 shows a typical plot of output power, PAE, and gain versus input power at 5 GHz and 10 V, while Figs. 33–35 show similar performances at 15, 20, and 28 V. Output powers of 27 dBm (1/2 W) to 28.9 dBm (3/4 W) were achievable with PAEs of 30% to 42% at lower voltages and lower frequencies, dropping with higher voltages and higher frequencies as the gain rolls off. Unlike simulations, there was no apparent increase in output power from 20 V to 28 V, just a corresponding drop in efficiency. Nonlinear simulations predicted 29 dBm (0.8 W) to 31 dBm (1.25 W) with 40% to 50% PAE at 10 V dropping significantly with voltage and frequency. Again, measuring unmatched HEMTs from the same wafer could be helpful in explaining the performance difference between measured and simulated. As with the distributed amplifier, small signal gain of the feedback amplifier generally matched better than the nonlinear performance.

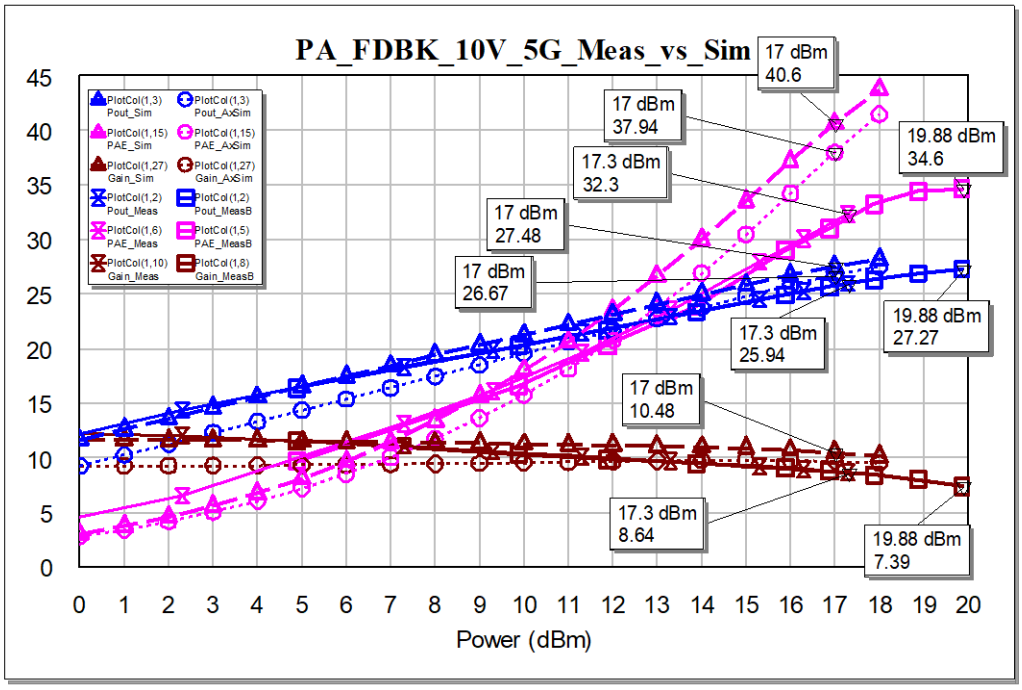

Fig. 32 Measured performance (solid) vs. simulations (dash) one-stage 0.44-mm broadband amp (10 V, 5 GHz)

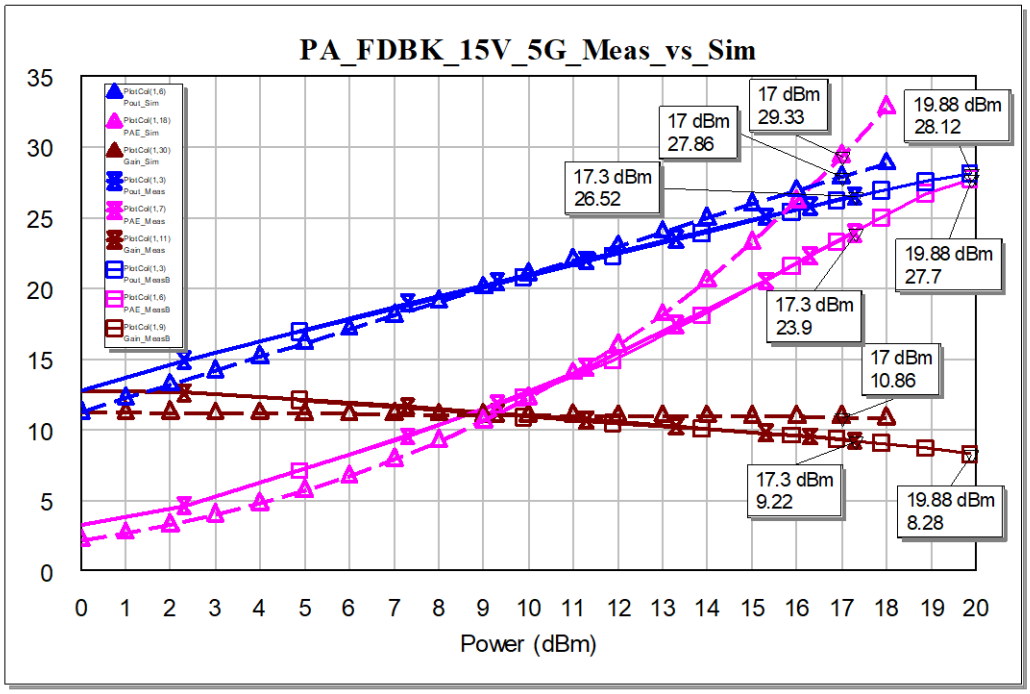

Fig. 33 Measured performance (solid) vs. simulations (dash) one-stage 0.44-mm broadband amp (15 V, 5 GHz)

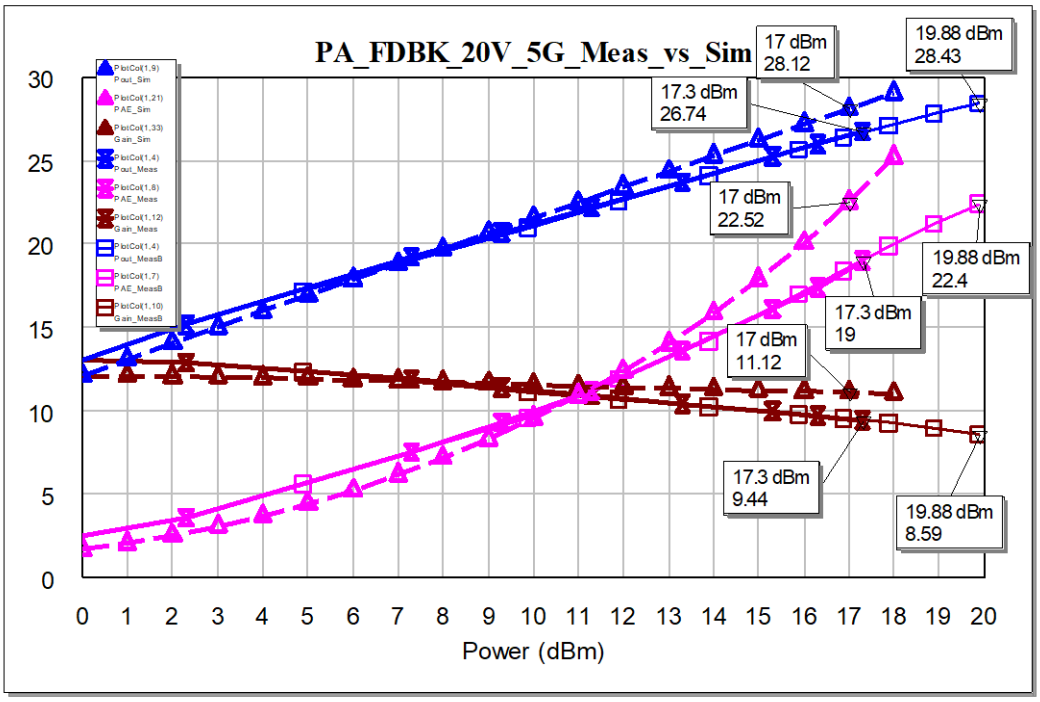

Fig. 34 Measured performance (solid) vs. simulations (dash) one-stage 0.44-mm broadband amp (20 V, 5 GHz)

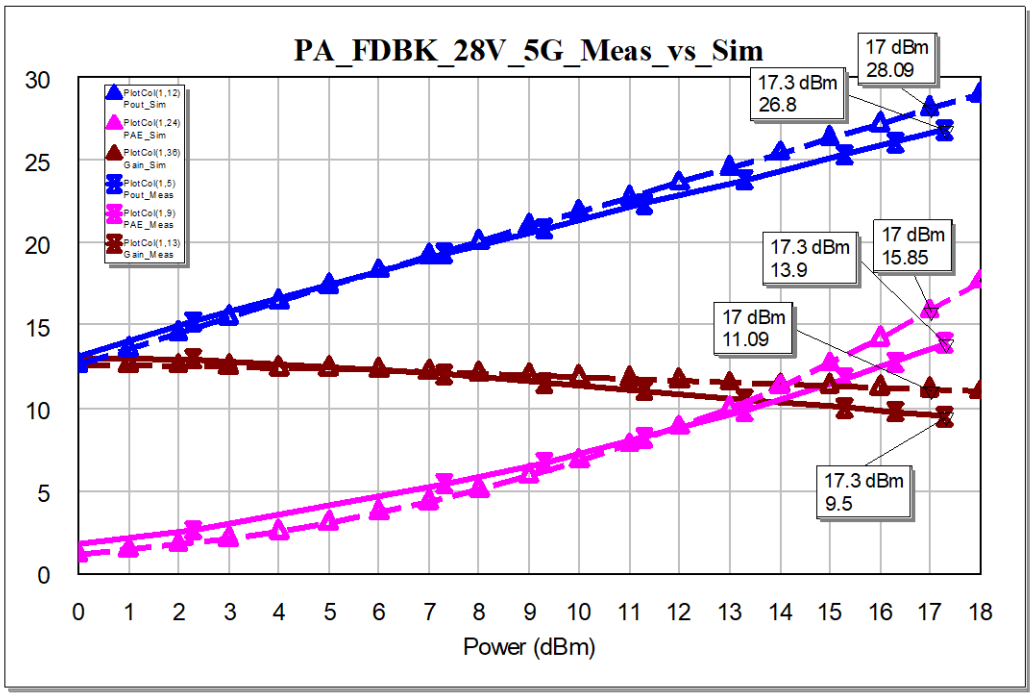

Fig. 35 Measured performance (solid) vs. simulations (dash) one-stage 0.44-mm broadband amp (28 V, 5 GHz)

7. Conclusion

Several MMIC designs were fabricated under an AFRL-sponsored Qorvo 0.25-µm GaN wafer run to demonstrate the performance, bandwidth, capability, versatility, and applicability of GaN for compact, efficient, microwave circuit designs.

The distributed amplifier demonstrated extremely broad band gain to 25 GHz, with reasonable output power and efficiency. Varying the output DC bias can optimize the output power and efficiency of these 0.25-µm GaN HEMT designs, though less power was measured than expected. Best efficiencies were at 10 V, with only slightly more output power at 15 or 20 V of bias. Nearly 1/2 W of output power was measured at 3, 5, and 7 GHz with about 25% PAE at 10 V DC.

The broadband feedback amplifier formed the driver stage of a two-stage PA. It was tested as a standalone compact one-stage amplifier, which similarly measured at lower output power than expected as with the DA design. It had been expected to produce nearly 1 W to easily drive the 1.75-mm second-stage amplifier, but measured closer from 0.5 W to 0.75 W at 3, 5, and 7 GHz with biases of 10, 15, and 20 V. Efficiency was very good at 10 V, with 30% to 42% at the measured frequencies, dropping in efficiency but increasing slightly in output power with DC biases of 15 and 20 V. There was little increase in output power at 28 V. In the two-stage PA design, two high-pass, lumped-element components were added to flatten the overall gain and provide a DC bias path to the drain of the broadband first-stage amplifier while DC blocking the gate of the second stage. A redesign with a larger feedback amplifier might improve the two-stage efficiency with minor risk as the design was stable and demonstrated good broadband gain.

A 1.75-mm HEMT was used for the one- and two-stage broadband 3–7 GHz PAs. As a one-stage, the amplifier had good output power and efficiency, matching simulations quite well. Early simulations with a Generation 1 HEMT model predicted higher output power than a more recent Generation 2 HEMT model, which more closely modeled the actual device performance. Over the 4–6 GHz midband, the one-stage amplifier produced 5.9 W to 6.7 W with PAE of 54% to 56%. Efficiencies were higher at lower voltages of 15 and 20 V, but output powers were lower. At 15-V DC bias, output power at 4–6 GHz was 3.5 W to 4.9 W with 57% to 69% PAE in class AB amplifier operation.

The gain slope with frequency of the 1.75-mm PA stage was flattened by the use of a broadband feedback amplifier driver stage with a simple high-pass filter interstage match. At 5 GHz, the two-stage performance was good, but the first stage was compressing earlier than expected. Though the first-pass, two-stage design

demonstrated reasonable performance, a redesign of the first stage could improve the overall performance.

Other designs include a TR switch that was designed for operation to 18 GHz. Using GaN HEMT switches increases the linear operating range of TR switches over previous gallium arsenide designs. The need to reduce the HEMT switch sizes to increase operation to 18 GHz sacrifices power handling capability and increases insertion loss. Small signal parameters match well with the simulations, with less than 1.5 dB measured insertion loss to 12 GHz, about 0.3 dB higher than initial simulations.

Passive power combiner circuits with isolation resistors that can handle the high powers of GaN amplifiers were fabricated. A simple 3–6 GHz single-stage passive Wilkinson coupler using a mesa resistor for isolation matched simulated small signal parameters; likewise, for a broadband two-stage 0.5–3 GHz Wilkinson coupler designed by Dana Sturzebecher of Qorvo. Power performance of these couplers have not been performed yet, but would need packaging of the die for high power tests.

Another interesting design demonstrating integration potential was the VCO, which demonstrated a compact 15-GHz VCO circuit. Tuning range and oscillation frequency match simulations very well. Output power was a reasonable 50 mW, though previous simulations (Generation 1 models) predicted up to 100 mW.

There are some standalone HEMT devices from the fabrication run that can be evaluated and tested to determine if normal process variation helps explain any differences between measurements and simulations. Those results could be used for future redesigns to improve performance of these designs, or others using the same 0.25-µm Qorvo GaN process. The plan is to obtain and test some of these HEMTs, which would be documented in a future technical report.

Prior technical reports provide more detail of the MMIC designs that were tested for this report.[1–3]

References

1. Penn JE. Gallium nitride (GaN) monolithic microwave integrated circuit (MMIC) designs submitted to Air Force Research Laboratory (AFRL)-sponsored Qorvo fabrication. Aberdeen Proving Ground (MD): Army Research Laboratory (US); 2017 July. Report No.: ARL-TN-0835.

2. Penn JE. Gallium nitride monolithic microwave integrated circuit designs using 0.25-μm Qorvo process. Aberdeen Proving Ground (MD): Army Research Laboratory (US); 2017 July. Report No.: ARL-TN-0836.

3. Penn JE. Broadband 0.25-μm gallium nitride (GaN) power amplifier designs. Aberdeen Proving Ground (MD): Army Research Laboratory (US); 2017 Aug. Report No.: ARL-TR-8091.

List of Symbols, Abbreviations, and Acronyms

AFRL	Air Force Research Laboratory
ARL	US Army Research Laboratory
Cgd	gate-drain capacitance
DA	distributed amplifier
DC	direct current
EM	electromagnetic
EW	electronic warfare
GaN	gallium nitride
GS	ground signal
GSG	ground-signal-ground
HEMT	high-electron-mobility transistor
MIM	metal-insulator-metal
MMIC	monolithic microwave integrated circuit
PA	power amplifier
PAE	power-added efficiency
PDK	process design kit
RF	radio frequency
SiC	silicon carbide
SPDT	single-pole, double-throw
TR	transmit/receive
VCO	voltage-controlled oscillator

1 (PDF)	DEFENSE TECHNICAL INFORMATION CTR DTIC OCA
2 (PDF)	DIR ARL IMAL HRA RECORDS MGMT RDRL DCL TECH LIB
1 (PDF)	GOVT PRINTG OFC A MALHOTRA
12 (10 PDF) (2 HC)	DIR USARL RDRL SER P AMIRTHARAJ RDRL SER E R DEL ROSARIO (1 HC) A DARWISH A HUNG T IVANOV P GADFORT K MCKNIGHT J PENN (1 HC) E VIVEIROS J WILSON